Endothelial cell–restricted disruption of *FoxM1* impairs endothelial repair following LPS-induced vascular injury

You-Yang Zhao,[1] Xiao-Pei Gao,[1] Yidan D. Zhao,[1] Muhammad K. Mirza,[1] Randall S. Frey,[1] Vladimir V. Kalinichenko,[2] I-Ching Wang,[3] Robert H. Costa,[3] and Asrar B. Malik[1]

[1]Department of Pharmacology, University of Illinois College of Medicine, Chicago, Illinois, USA. [2]Department of Medicine, The University of Chicago, Chicago, Illinois, USA. [3]Department of Biochemistry and Molecular Genetics, University of Illinois College of Medicine, Chicago, Illinois, USA.

Recovery of endothelial integrity after vascular injury is vital for endothelial barrier function and vascular homeostasis. However, little is known about the molecular mechanisms of endothelial barrier repair following injury. To investigate the functional role of forkhead box M1 (FoxM1) in the mechanism of endothelial repair, we generated endothelial cell–restricted FoxM1-deficient mice (*FoxM1* CKO mice). These mutant mice were viable and exhibited no overt phenotype. However, in response to the inflammatory mediator LPS, *FoxM1* CKO mice displayed significantly protracted increase in lung vascular permeability and markedly increased mortality. Following LPS-induced vascular injury, *FoxM1* CKO lungs demonstrated impaired cell proliferation in association with sustained expression of $p27^{Kip1}$ and decreased expression of cyclin B1 and Cdc25C. Endothelial cells isolated from *FoxM1* CKO lungs failed to proliferate, and siRNA-mediated suppression of FoxM1 expression in human endothelial cells resulted in defective cell cycle progression. Deletion of FoxM1 in endothelial cells induced decreased expression of cyclins, Cdc2, and Cdc25C, increased $p27^{Kip1}$ expression, and decreased Cdk activities. Thus, FoxM1 plays a critical role in the mechanism of the restoration of endothelial barrier function following vascular injury. These data suggest that impairment in FoxM1 activation may be an important determinant of the persistent vascular barrier leakiness and edema formation associated with inflammatory diseases.

Introduction

The endothelial monolayer at the interface between extravascular space and blood plays a crucial role in vascular homeostasis (1). The endothelial monolayer helps to maintain the antithrombotic and antiinflammatory state of the microvascular bed, and it additionally controls the tone and proliferative state of the underlying vascular smooth muscle cells. In pathologic situations, such as the initiation and progression of atherosclerosis and acute lung injury (ALI), vascular endothelial injury and increased permeability of the barrier promote the extravasation of neutrophils and monocytes across the vessel wall (2, 3). This loss of endothelial barrier function is associated with severe consequences: tissue edema formation, thrombus formation, neointimal thickening, and abnormal responses to endothelium-dependent agonists (4–6). Intractable endothelial injury characterized by persistently increased lung vascular permeability is a hallmark of ALI (7). Reversibility of endothelial injury reflects the severity of injury itself as well as the capacity of cells to undergo the repair necessary for reannealing the endothelial barrier. However, the molecular mechanisms that regulate endothelial cell proliferation and barrier repair following vascular injury are poorly understood.

Forkhead box M1 (FoxM1 or FoxM1B; previously known as HFH-11/Trident/Win/MPP2) is a member of the mammalian fox family of transcription factors that share homology in the winged helix or forkhead DNA–binding domain (8, 9). FoxM1 is expressed during cellular proliferation and is silenced in terminally differentiated cells (10–12). During liver regeneration, FoxM1 is essential for hepatocyte DNA replication and entry into mitosis (13). Mouse hepatocytes deficient in FoxM1 failed to develop hepatocellular carcinomas in response to carcinogens as a result of impaired hepatocyte proliferation (14). Another study using a transgenic mouse model demonstrated that overexpression of FoxM1 accelerates the proliferation of distinct pulmonary cell types following butylated hydroxytoluene–induced lung injury (15). Previous studies have not addressed whether FoxM1 has a role in the mechanism of repair of the endothelial barrier following vascular injury, as the *FoxM1*-null mutation causes embryonic lethality due to impaired execution of mitosis (16). Studies demonstrate that FoxM1 is essential for the expression of cell division cycle 25A (Cdc25A) phosphatase and diminishment of the nuclear accumulation of the cyclin-dependent kinase inhibitor proteins $p21^{Cip1}$ and $p27^{Kip1}$ required for progression into DNA replication (13, 14). During the G2/M transition, FoxM1 regulates transcription of Cdc25B phosphatase responsible for stimulating cyclin-dependent kinase 1 (Cdk1) activity and inducing expression of aurora B kinase, survivin, and polo-like kinase 1, which in turn phosphorylates substrates essential for mitosis (13, 14, 17–19). Herein, using mice with endothelial cell–restricted *FoxM1* deficiency (*FoxM1* CKO mice), we addressed the possibility that FoxM1 regulates endothelial cell proliferation after injury and thereby promotes the recovery of lung microvasculature endothelial barrier function. *FoxM1* CKO mice

Nonstandard abbreviations used: ALI, acute lung injury; BW, body weight; Cdc25A, cell division cycle 25A; Cdk1, cyclin-dependent kinase 1; FoxM1, forkhead box M1; *FoxM1* CKO, endothelial cell–restricted *FoxM1*-deficient (mice); HMEC-1, human microvascular endothelial cell(s) 1; $K_{f,c}$, filtration coefficient; MCP-1, monocyte chemoattractant protein-1; MIP-1α, macrophage inflammatory protein 1α; QRT-PCR, quantitative real-time RT-PCR; Rb, retinoblastoma.

Conflict of interest: The authors have declared that no conflict of interest exists.

Citation for this article: *J. Clin. Invest.* **116**:2333–2343 (2006). doi:10.1172/JCI27154.

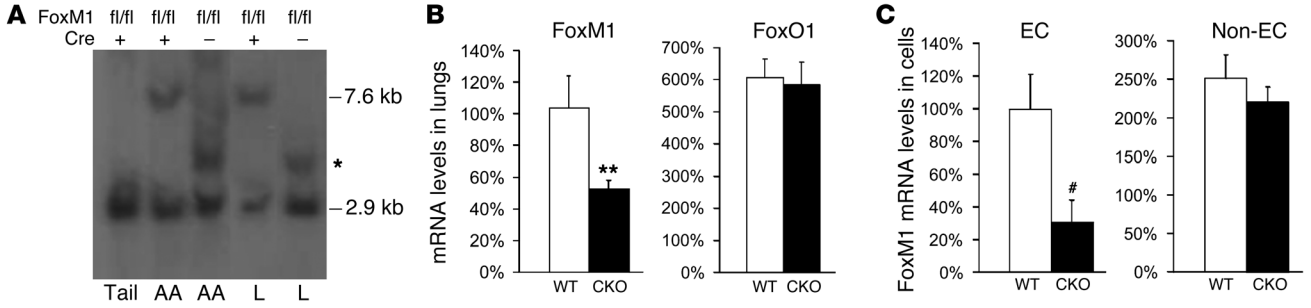

Figure 1

Mouse model of endothelial cell–restricted deletion of *FoxM1*. (**A**) Southern blot demonstrating recombination of the *FoxM1* floxed allele in endothelial cell–enriched tissues. Mouse genomic DNA (15 μg /lane) was digested with Bgl II and XbaI. The blots were probed with 3′ probe as described (13). *Tie2* promoter/enhancer-driven *Cre* expression created a predicted 7.6-kb band in the aorta and lungs. The pseudogene band is indicated by an asterisk. (13). fl, *FoxM1* floxed allele; AA, aorta; L, lung. (**B**) Quantitative analysis of mRNA expression of FoxM1 and FoxO1 by QRT-PCR. RNA was extracted from lungs of either *FoxM1* WT or *FoxM1* CKO mice. mRNA expression of FoxM1 and FoxO1 was normalized to mouse cyclophilin mRNA. There were no differences in FoxM1 mRNA levels in mice with the 3 genotypes $FoxM1^{+/+}$, $FoxM1^{fl/+}$, and $FoxM1^{fl/fl}$; therefore, all these mice were referred to as WT mice. Data are expressed as mean ± SD, $n = 3$. $^{**}P < 0.05$. CKO, *FoxM1* CKO. (**C**) Quantitative analysis of FoxM1 expression in population of cells either enriched or depleted of endothelial cells. RNA was extracted from an endothelial cell–enriched primary culture (EC, passage 0) isolated from mouse lungs or from nonendothelial cell primary cultures (non-EC, passage 4), fibroblasts, and epithelial cells. Approximately 70% reduction of FoxM1 mRNA levels was detected in *FoxM1* CKO EC and not in *FoxM1* CKO non-EC ($n = 3$), indicating endothelial cell–specific knockdown of FoxM1. $^{\#}P < 0.01$. $n = 3$.

were generated using *Tie2* promoter/enhancer-driven *Cre* transgenic mice. Following LPS-induced lung microvascular injury, *FoxM1* CKO mice exhibited markedly impaired endothelial barrier recovery due to defective endothelial cell proliferation associated with increased expression of $p27^{Kip1}$ and decreased expression of cyclin B1 and Cdc25C. *FoxM1* CKO mice also showed increased mortality in response to LPS challenge in association with severe pulmonary edema. These data demonstrate for what we believe is the first time that FoxM1 is essential in regulating the proliferation of endothelial cells subsequent to an inflammatory insult and that it thereby plays an important role in reestablishing endothelial barrier integrity following vascular injury. The results point to the value of therapeutic strategies targeting FoxM1 to promote endothelial barrier reannealing and resolve inflammation.

Results

Endothelial cell–specific disruption of FoxM1. To gain insights into the function of FoxM1 in endothelial repair following vascular injury, we inactivated FoxM1 in the mouse endothelium. Mice carrying a *FoxM1* gene in which exons 4–7 were flanked by 2 *loxP* sites (13) were bred with *Tie2* promoter/enhancer-driven *Cre* transgenic mice (20). *Tie2* promoter/enhancer-driven *Cre* expression induced endothelial cell–specific deletion of mouse *FoxM1 loxP/loxP*-targeted allele by removing the entire winged-helix DNA–binding and C terminal transcriptional activation domains (13). As shown in Figure 1A, the predicted recombination-derived 7.6-kb band was identified in Southern blots only in endothelial cell–rich tissues such as aorta and lung from *FoxM1* CKO. The WT 2.9-kb band was more prominent in cells that did not express *Cre*. Quantitative real-time RT-PCR (QRT-PCR) revealed a 50% reduction in FoxM1 mRNA expression in *FoxM1* CKO lungs whereas expression of FoxO1, a ubiquitously expressed *Fox*, was unaffected (Figure 1B). As shown in Figure 1C, we observed 70% reduction of FoxM1 mRNA expression in primary cultures of endothelial cells isolated from *FoxM1* CKO lungs but not in nonendothelial cells (fibroblasts and epithelial cells). As the primary culture of *FoxM1* CKO endothelial cells was assessed as 90% pure, the efficiency of FoxM1 deletion was greater than 90%, a level comparable to that given in other reports of *Tie2-Cre* endothelial-specific gene deletions (20–22).

FoxM1 CKO mice have normal cardiovascular systems and basal lung vascular permeability. Unlike the *FoxM1*-null mutation mice (16, 23), approximately 80% of *FoxM1* CKO were viable and indistinguishable from their WT littermates. *FoxM1* CKO mice grew to adulthood, living as long as WT mice (≥ 18 months). *FoxM1* CKO hearts and lungs from adult mice (4–5 months) were histologically normal (Figure 2E and data not shown); heart/body weight (BW) ratio was not different from that of WT (data not shown). To evaluate endothelial barrier function, we quantified microvascular permeability in the murine isolated perfused lung model (24, 25). The basal lung capillary filtration coefficient ($K_{f,c}$) of *FoxM1* CKO was similar to that of WT (Figure 2A).

FoxM1 is required for endothelial barrier reannealing following LPS-induced vascular injury. To determine whether FoxM1 was induced after the onset of vascular injury, we challenged mice by i.p. injection with LPS, the gram-negative bacterial cell wall component, to induce ALI (24, 26, 27). QRT-PCR revealed a 4-fold increase of FoxM1 mRNA expression in WT lungs 3 days after LPS challenge at a dose of 5 mg/kg BW (Figure 3A). The induction was not detected until day 2 and peaked at day 3 after LPS challenge (Figure 3A and Supplemental Figure 1; supplemental material available online with this article; doi:10.1172/JCI27154DS1). Recruitment of inflammatory cells into lungs and vascular leakage are known to occur as early as 3 hours after LPS challenge with maximal lung microvascular injury observed at approximately 24 hours (24, 28, 29). Thus, the time course of FoxM1 expression (Figure 3A) paralleled the recovery phase of LPS-induced injury. In contrast to WT lungs, there was a significantly lower FoxM1 expression detected at day 3 and day 4 after LPS challenge in *FoxM1* CKO lungs (Figure 3A), reflecting the presence of FoxM1 expression in the nonendothelial cell population. In addition, 2 other inflammatory mediators, TNF-α and H_2O_2, significantly induced FoxM1 mRNA in primary cultures of endothelial cells isolated from WT mouse lungs (Figure 3B).

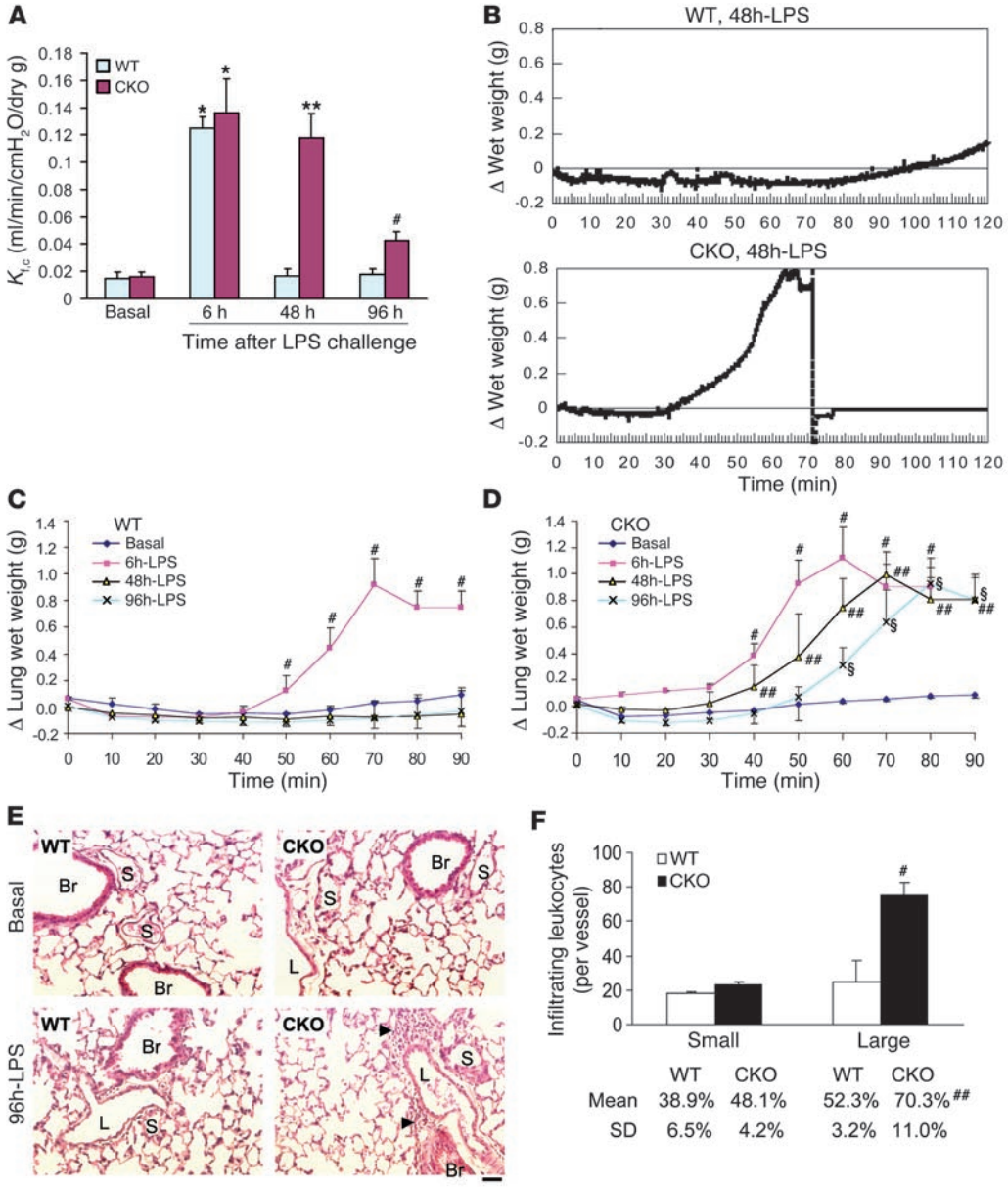

Figure 2

Impaired lung vascular endothelial barrier reannealing following LPS-induced microvascular injury in *FoxM1* CKO mice. (**A**) Time course of increase in lung microvessel permeability as measured by $K_{f,c}$. Basal, 0.2 ml PBS; LPS, 5 mg/kg BW. Data are expressed as mean ± SD, n = 3–5 per group. $^{*}P < 0.001$ versus basal; $^{**}P < 0.001$, CKO versus WT; $^{\#}P < 0.05$, CKO versus WT. (**B**) Representative graphs of mouse lung wet weights continuously recorded during measurement of microvessel permeability. 48h-LPS, 48 hours after LPS challenge. (**C** and **D**) Time course of loss of isogravimetric state of lungs (edema formation) obtained from mouse lungs at indicated times after LPS challenge. WT (**C**) and *FoxM1* CKO mice (**D**) are represented. Points indicate mean ± 1 SD, n = 3–5 mice per group. $^{\#}P < 0.05$ WT or CKO 6 hours after LPS challenge (6h-LPS) versus basal; $^{\#\#}P < 0.05$ CKO 48 hours after LPS challenge (48h-LPS) versus CKO basal or WT 48 hours after LPS challenge; $^{\S}P < 0.05$ CKO 96 hours after LPS challenge (96h-LPS) versus CKO basal or WT 96 hours after LPS challenge. (**E**) Representative micrographs of H&E staining show perivascular leukocyte infiltration in *FoxM1* CKO lungs 96 hours after LPS challenge (5 mg/kg). Arrows indicate leukocyte infiltration. Br, bronchia; S, small vessels (<150 μm in diameter); L, large vessels (>150 μm in diameter). Scale bar: 50 mm. (**F**) Quantitative analysis of infiltrating leukocytes in lungs at 96 hours after LPS challenge. Bar graphs show infiltrating leukocytes in vessels of different diameters. Percentages of vessels of different diameters exhibiting leukocyte infiltration are shown. Data are expressed as mean ± SD, n = 3–4. $^{\#}P < 0.05$ versus WT (infiltrating leukocytes per vessel); $^{\#\#}P < 0.05$ versus WT (% of vessels).

As seen in the acute phase of ALI in humans (7), endothelial injury induced by LPS is characterized by endothelial cell apoptosis and increased endothelial permeability (24, 28–30). We therefore assessed these responses in *FoxM1* CKO lungs. After LPS challenge, there was no significant difference in the level of apoptosis in lung sections of *FoxM1* CKO and WT mice at either day 1 (the peak of apoptosis response in both groups; Figure 4, A and B) or at later time points (data not shown). As shown in Figure 4C, both WT

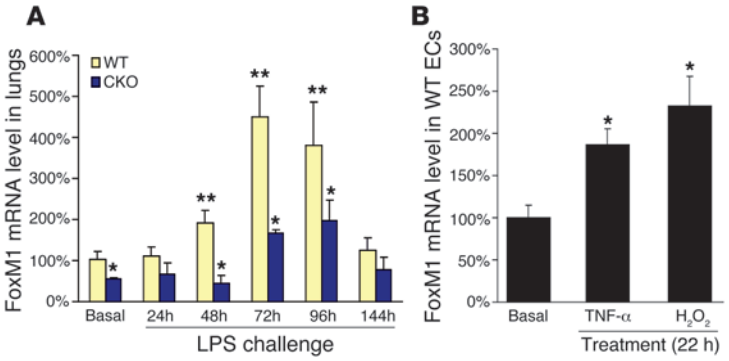

Figure 3
Time course of FoxM1 expression following LPS-induced lung microvascular injury. (**A**) Quantitative analysis of FoxM1 mRNA levels in mouse lungs by QRT-PCR. Total RNA was extracted from lungs collected from either WT or *FoxM1* CKO mice after LPS exposure (5 mg/kg BW) at indicated times. FoxM1 mRNA levels were normalized to cyclophilin. Data are expressed as mean ± SD, n = 3–4. *P < 0.05 WT versus CKO; **P < 0.05 versus basal WT. (**B**) FoxM1 mRNA expression in endothelial cell–enriched primary cultures isolated from WT mouse lungs. Total RNA was extracted from endothelial cell–enriched primary cultures (passage 2) treated with either PBS (basal), 1,000 U/ml of recombinant mouse TNF-α, or 10 μM of H_2O_2 for 22 hours. Data are expressed as mean ± SD, n = 3. *P < 0.05.

and *FoxM1* CKO lungs exhibited similar increases in myeloperoxidase activity 6 hours after LPS challenge, indicating no difference in lung neutrophil sequestration. To determine the in vivo consequences of inhibiting post-LPS FoxM1 expression on vascular permeability, we isolated lungs from mice to quantify endothelial barrier function by measuring $K_{f,c}$ and edema formation in isogravimetric lung preparation (24, 25). Mice were injected i.p. with either PBS (0.2 ml, pH 7.4) or LPS (5 mg/kg BW in 0.2 ml PBS), and lungs were evaluated at 6, 48, and 96 hours thereafter. We have previously shown that LPS at this concentration induces maximal increase of $K_{f,c}$ at 6 hours in WT lungs (24). In the present study, we observed that $K_{f,c}$ values at 6 hours were not significantly different in *FoxM1* CKO and WT lungs (Figure 2A). In WT lungs, $K_{f,c}$ returned to baseline level at 48 hours; however, $K_{f,c}$ in *FoxM1* CKO lungs remained significantly elevated at 48 hours and 96 hours. In addition, we recorded lung wet weight changes after LPS challenge as a measure of edema formation. As demonstrated by the precipitous rise in lung wet weight, edema formation was a prominent feature of *FoxM1* CKO lungs beginning at 48 hours and continuing through 96 hours, a response not seen in WT lungs (Figure 2, B–D). Thus, LPS induced similar vascular injury in *FoxM1* CKO and WT lungs as shown by the increase in $K_{f,c}$ at 6 hours, but the critical difference seen in *FoxM1* CKO lungs was the persistent vascular injury resulting in increased vascular permeability. We also observed perivascular leukocyte sequestration (primarily around large vessels) in *FoxM1* CKO lungs 96 hours after LPS challenge;

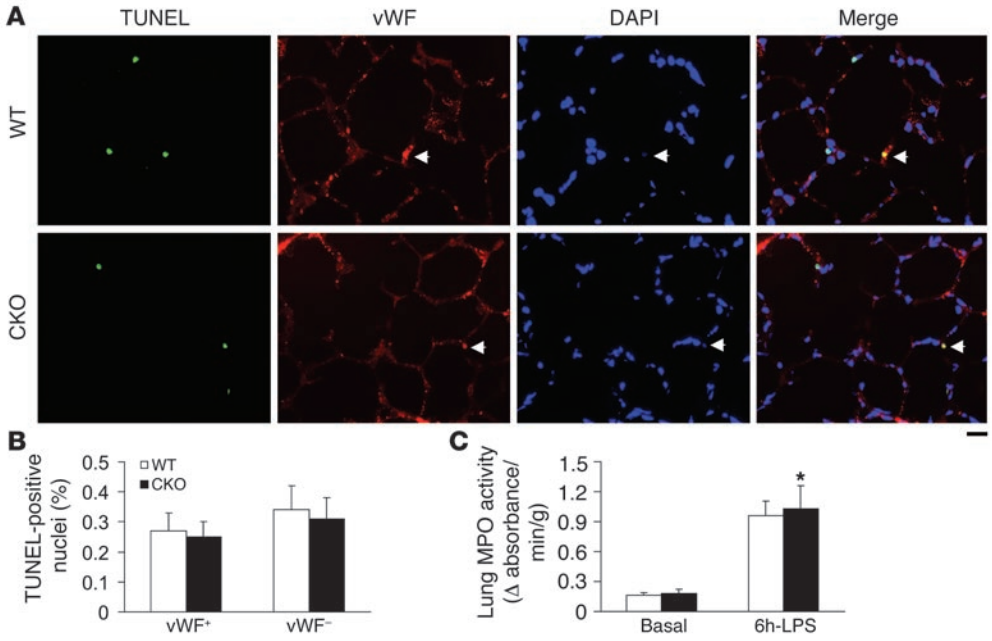

Figure 4
FoxM1 CKO mice exhibit endothelial apoptosis and lung neutrophil sequestration similar to that of WT mice in the early period following LPS challenge. (**A**) Representative micrographs of TUNEL staining. Cryosections of lungs (3- to 5-μm thick) collected 24 hours after LPS challenge were stained with FITC-conjugated TUNEL to identify apoptotic cells and anti-vWF antibody to identify endothelial cells; nuclei were counterstained with DAPI. Arrows, TUNEL+vWF+ cells. Scale bar: 25 mm. (**B**) Graphic representation of apoptotic endothelial cells and nonendothelial cells in *FoxM1* CKO and WT lungs 24 hours after LPS challenge (5 mg/kg BW). The number of TUNEL-positive nuclei and vWF-positive cells from 3 to 4 consecutive cryosections from each mouse lung were averaged. Data are expressed as mean ± SD, n = 3–4 mice per group. There is no difference between WT and FoxM1 CKO. (**C**) Lung tissue myeloperoxidase (MPO) activity during basal period and 6 hours after LPS challenge (5 mg/kg BW). Data are expressed as mean ± SD, n = 4 mice per group. *P > 0.1 versus WT. Although there is a significant increase in MPO activity in mouse lungs 6 hours following LPS challenge, both WT and *FoxM1* CKO lungs exhibit similar MPO activities, indicating a similar extent of polymorphonuclear leukocyte sequestration.

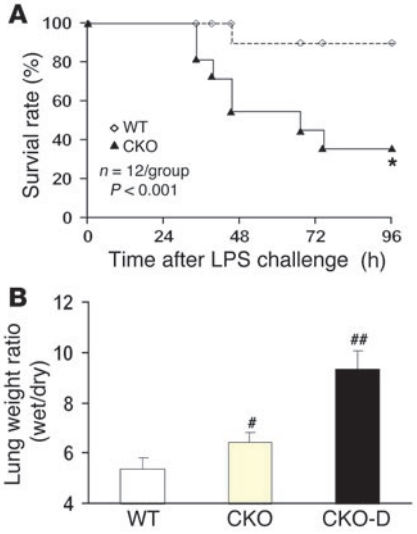

Figure 5
Increased mortality in *FoxM1* CKO mice following LPS challenge. (**A**) Survival rate following LPS challenge. Mice were challenged i.p. with 12 mg/kg BW of LPS and housed under normal conditions. Approximately 70% of the *FoxM1* CKO mice died from day 2 to day 4 after LPS challenge whereas only about 10% of WT mice died in this same period. Differences in the survival rates between the WT and CKO groups after LPS challenge were significant by Peto-Peto-Wilcoxon test. n = 11 mice per group. $^{*}P < 0.001$. (**B**) Graphic representation of development of lung edema in *FoxM1* CKO mice following LPS challenge (12 mg/kg). Lungs were collected either at 48 hours after LPS challenge (WT and CKO) or in some mice at day 2 just prior to their deaths (CKO-D). Data are expressed as mean ± SD. n = 3–5, $^{\#}P < 0.05$ versus WT; $^{\#\#}P < 0.01$ versus WT.

however, in WT lungs, this response was almost fully resolved by 96 hours (Figure 2, E and F). Strikingly, a higher dosage of LPS (12 mg/kg BW) resulted in a significantly greater mortality rate in *FoxM1* CKO compared with WT mice (Figure 5A). We observed that 70% of *FoxM1* CKO died within 96 hours of LPS treatment; in contrast, only 10% of WT mice died within this time (Figure 5A). Severe fulminant pulmonary edema was an important determinant of death in *FoxM1* CKO mice (Figure 5B).

Deletion of FoxM1 in bone marrow cells and generation of proinflammatory cytokines and chemokines do not contribute to defective vascular repair in FoxM1 CKO mice. *Tie2* promoter/enhancer-driven *Cre* expression may also induce the deletion of the *FoxM1* gene in hematopoietic cells, which could thus interfere with the vascular repair process (31). As shown in Figure 6, FoxM1 expression was not different in *FoxM1* CKO bone marrow cells compared with WT. However, it cannot be ruled out that FoxM1 might be deleted in a small subpopulation of hematopoietic cells in *FoxM1* CKO. To determine whether *FoxM1* CKO hematopoietic cells contributed to defective endothelial barrier repair following LPS challenge, WT bone marrow cells were transplanted into lethally irradiated *FoxM1* CKO mice. FACS analysis demonstrated approximately 80% reconstitution of *FoxM1* CKO bone marrow at 3 weeks after transplantation (Figure 6A). Transplantation of WT bone marrow in *FoxM1* CKO mice failed to prevent the sustained increase of lung vascular permeability after LPS challenge (Figure 6B); thus, deletion of FoxM1 in hematopoietic cells does not contribute to defect in endothelial repair in *FoxM1* CKO lungs.

As increased expression of proinflammatory mediators may also contribute to increased vascular permeability in *FoxM1* CKO lungs, we investigated this possibility by determining the expression of several mediators in lungs following LPS challenge. We observed no difference in expression of various cytokines and chemokines between WT and *FoxM1* CKO lungs after LPS challenge (Table 1).

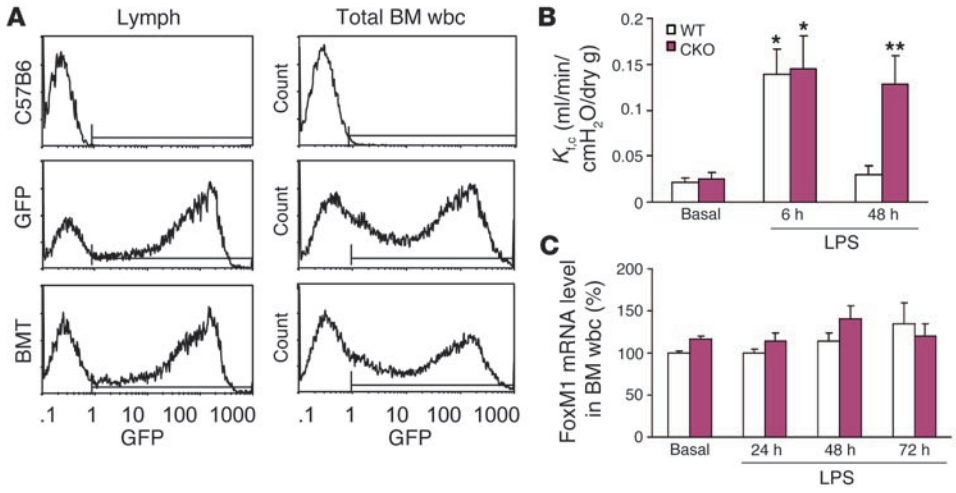

Figure 6
Failure of WT bone marrow cells to rescue the vascular repair defect in *FoxM1* CKO mice following LPS challenge. (**A**) FACS analysis of GFP-positive bone marrow lymphocytes (lymph) and total white blood cells. At 3 weeks following transplantation of WT bone marrow cells isolated from GFP-transgenic mice, bone marrow cells were isolated from reconstituted *FoxM1* CKO and red blood cells were lysed prior to FACS analysis. Bone marrow white blood cells isolated from C57B6 mice and GFP-transgenic mice were used as negative and positive controls, respectively. Approximately 80% of bone marrow reconstitution was achieved. BMT, WT bone marrow cell–transplanted *FoxM1* CKO. (**B**) Sustained increase in lung microvessel permeability in WT bone marrow cell–transplanted *FoxM1* CKO following LPS challenge. At 5 weeks following WT bone marrow transplantation, lungs from WT or *FoxM1* CKO mice were isolated for $K_{f,c}$ measurement. Data are expressed as mean ± SD, n = 3–5 per group. $^{*}P < 0.001$ versus basal; $^{**}P < 0.001$, CKO versus WT. Basal, 0.2 ml PBS. CKO, FoxM1 CKO mice reconstituted with WT bone marrow cells. (**C**) Quantitative analysis of FoxM1 mRNA expression in bone marrow cells. Bone marrow white blood cells were isolated from either WT or *FoxM1* CKO at the indicated time points following LPS challenge, and RNA was isolated for QRT-PCR analysis. FoxM1 mRNA levels were normalized to cyclophilin. Data are expressed as mean ± SD, n = 3 per group. In contrast to endothelial cells isolated from *FoxM1* CKO lungs, the white blood cells from *FoxM1* CKO bone marrow expressed FoxM1 at the same level as WT.

Table 1
Expression profiles of proinflammatory cytokines and chemokines in lungs following LPS challenge

	IL-1β		TNF-α		IFN-γ		MIP-1α		MCP-1	
	24 h	48 h	24 h	48 h	24 h	48 h	24 h	48 h	24 h	48 h
WT	2.1 ± 0.2	0.9 ± 0.04	1.1 ± 0.3	0.8 ± 0.1	15.3 ± 3.5	5.7 ± 0.6	4.2 ± 0.8	2.3 ± 0.3	11.0 ± 0.8	11.6 ± 2.1
CKO	2.4 ± 0.4	0.7 ± 0.06	1.2 ± 0.35	0.8 ± 0.05	17.0 ± 3.8	6.4 ± 0.8	4.8 ± 0.7	2.5 ± 0.3	14.5 ± 0.3	11.7 ± 2.8

Lungs were collected from WT or *FoxM1* CKO (CKO) mice at 24 or 48 hours following LPS challenge (5 mg/kg BW) and homogenized using RIPA buffer. A total of 25 μl of each lung lysate was used for the mouse Bio-Plex Cytokine Assay. Each value represents the expression level (pg/μg total lysate) of each cytokine or chemokine in the lung. Data are expressed as mean ± SD.

Deletion of FoxM1 in endothelial cells decreases cell proliferation after injury. We determined whether defective vascular repair in *FoxM1* CKO mice was attributed to decreased endothelial cell proliferation. Mice were challenged with LPS, and cell proliferation was measured by BrdU incorporation. WT lungs exhibited increased cellular proliferation that peaked at 72 hours (Figure 7, A and B), paralleling the time course of FoxM1 mRNA induction (Figure 3A). Although cellular proliferation in *FoxM1* CKO and WT lungs was comparable at 24 hours following LPS challenge, the response was significantly impaired in *FoxM1* CKO lungs at 48 and 72 hours (Figure 7B). This impairment was primarily the result of the defect in endothelial cell proliferation (Figure 7C and Supplemental Figure 2). In tissue from *FoxM1* CKO lungs, nuclear staining of $p27^{Kip1}$ protein, an inhibitor of cyclin-dependent kinases, was markedly increased in endothelial cells compared with WT endothelial cells after LPS challenge (Figure 8, A and B). Expression of $p27^{Kip1}$ was sustained in the *FoxM1* CKO lungs while its expression decreased in WT lungs in response to LPS (Figure 8C and Supplemental Figure 3). QRT-PCR also demonstrated a significant decrease in the expression of Cdc25C and cyclin B1 in *FoxM1* CKO lungs compared with WT following LPS challenge (Figure 8, D and E).

FoxM1 is required for endothelial cell proliferation. The reduced endothelial cell proliferation found in *FoxM1* CKO lungs suggests that FoxM1 plays a crucial role in vascular endothelial barrier reannealing. We addressed this question using endothelial cells isolated from either *FoxM1* CKO or WT mouse lungs. The growth of endothelial cells cultured from *FoxM1* CKO lungs was markedly reduced (Figure 9A). After 5–7 days in culture, *FoxM1* CKO endothelial cells were less than 20% confluent whereas WT cells reached more than 80% confluency. In contrast, primary cultures of nonendothelial cells from *FoxM1* CKO lungs, which retained the $FoxM1^{fl/fl}$ targeted allele, displayed similar growth rates compared with WT (data not shown).

To address mechanisms of the proliferative defect in *FoxM1* CKO endothelial cells, we transfected siRNA into human microvascular endothelial cells 1 (HMEC-1) in order to suppress FoxM1 expression (Figure 9B). FACS analysis showed significant accumulation of 4 N DNA content in HMEC-1 cultures treated with FoxM1 siRNA (Figure 9, C and D), suggesting a defect in progression from G2 into mitosis. FoxM1-depleted HMEC-1 also exhibited a polyploid (8 N) peak indicative of endoreduplication caused by entry into a second round of DNA replication without completion of mitosis (Figure 9, C and D). As also seen in *FoxM1* CKO lungs, the expression of $p27^{Kip1}$ was significantly upregulated and nuclear staining of $p27^{Kip1}$ was prominent in FoxM1-deficient endothelial cells (Figure 10, A and B). Both Cdk1 and Cdk2 activities were

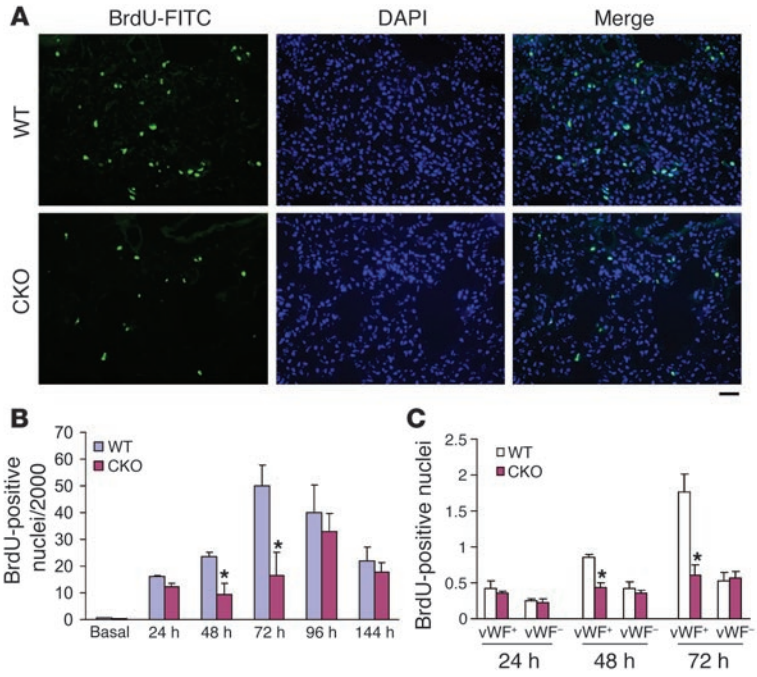

Figure 7
Decreased cell proliferation in *FoxM1* CKO lungs following LPS-induced lung microvascular injury. (**A**) Representative micrographs of BrdU immunostaining. Cryosections of lungs (3- to 5-μm thick), collected 72 hours after LPS challenge, were stained with FITC-conjugated anti-BrdU antibody to identify proliferating cells; nuclei were counterstained with DAPI. Scale bar: 25 mm. (**B**) Graphic representation of decreased BrdU incorporation in *FoxM1* CKO lungs and WT lungs at the indicated times following LPS challenge (5 mg/kg BW). From 3 to 4 consecutive cryosections from each mouse lung were examined, and the average number of BrdU-positive nuclei per 2,000 nuclei was used as the value for the mouse. Data are expressed as mean ± SD, n = 3–4 mice per time point. *P < 0.05 versus WT at 48 and 72 hours after LPS. There are few BrdU-positive nuclei (<1 BrdU positive nuclei per 2,000 nuclei) in both WT and *FoxM1* CKO lungs in the absence of LPS challenge. (**C**) Graphic representation of decreased proliferating endothelial cells (double-positive staining of vWF and BrdU) in *FoxM1* CKO lungs. Data are expressed as mean ± SD, percentage of total nuclei, n = 3–4 mice per time point per group. *P < 0.05 versus WT.

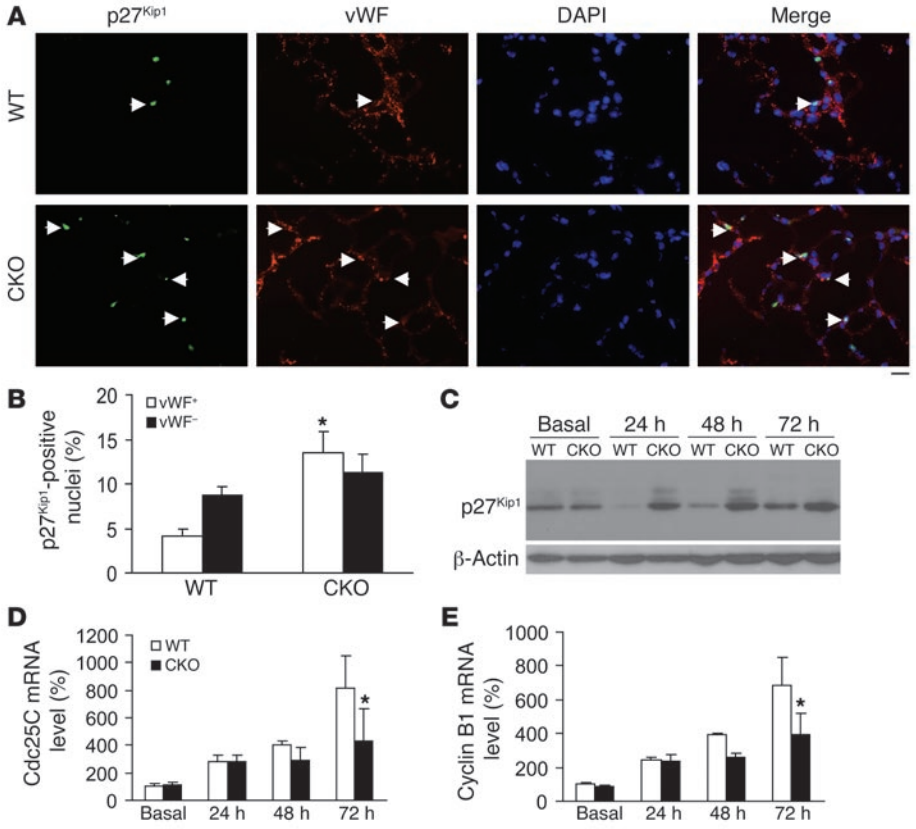

Figure 8

Increased nuclear staining and expression of $p27^{Kip1}$ and decreased expression of Cdc25C and cyclin B1 in *FoxM1* CKO lungs. (**A**) Representative micrographs of immunostaining of $p27^{Kip1}$ and vWF. Cryosections of lungs collected 24 hours after LPS challenge (5 mg/kg) were stained with antibodies against $p27^{Kip1}$ and vWF (marker for endothelial cells); nuclei were counterstained with DAPI. Arrows indicate $p27^{Kip1+}vWF^{+}$ cells. Scale bar: 25 μm. (**B**) Graphic representation of $p27^{Kip1}$-positive endothelial cells and nonendothelial cells. Data are expressed as mean ± SD, $n = 3–4$ mice per group. $^{*}P < 0.05$ versus WT. (**C**) Sustained expression of $p27^{Kip1}$ in *FoxM1* CKO lungs following LPS challenge (5 mg/kg). Protein (50 μg) from mouse lungs was loaded for each lane, the gel was electrophoresed, and proteins were transferred to PVDF and probed with monoclonal antibody against $p27^{Kip1}$. The same membrane was reprobed with a rabbit polyclonal antibody against β-actin as a loading control. The experiment was repeated 3 times with similar results. (**D** and **E**) Time course of expression of Cdc25C (**D**) and cyclin B1 (**E**) in lungs following LPS challenge (5 mg/kg). Total RNA was extracted from lungs collected from either WT mice or *FoxM1* CKO mice after LPS exposure (5 mg/kg BW) at the indicated times. Quantitative analysis of mRNA levels in mouse lungs was performed with QRT-PCR. Cdc25C and cyclin B1 mRNA levels were normalized to cyclophilin. Data are expressed as mean ± SD, $n = 3–4$. $^{*}P < 0.05$ versus WT.

markedly decreased in FoxM1-deficient endothelial cells (Figure 10C), and the set of genes essential for cell cycle progression, including those coding for several cyclins, Cdc2, and Cdc25C, were significantly decreased (Figure 10D). Taken together, these results demonstrate that FoxM1 is required for endothelial cell proliferation and is therefore crucial for the recovery of endothelial barrier function after vascular injury.

Discussion

We have identified the essential role of FoxM1 in mediating endothelial repair following vascular injury using a mouse model of endothelial cell–restricted *FoxM1* deletion. Mice with endothelial cell–specific deficiency of FoxM1 were viable and had normal basal endothelial barrier function. Lung microvascular permeability increased in these mice within 6 hours in response to the inflammatory mediator LPS. This response was similar to that of WT mice, as was LPS-induced endothelial cell apoptosis and neutrophil sequestration in the lungs. Strikingly, *FoxM1* CKO exhibited a marked impairment in endothelial barrier repair. We also found a significant increase in mortality following LPS-induced injury in these mice. We attributed the persistent increase in lung microvascular permeability in the LPS-challenged *FoxM1* CKO mice to defective endothelial cell proliferation that was associated with sustained expression of $p27^{Kip1}$ and decreased expression of cyclin B1 and Cdc25C. Together, these results demonstrate a crucial role of FoxM1 in restoring lung endothelial barrier integrity through its ability to activate endothelial cell proliferation in response to vascular endothelial injury.

There are several possible explanations for the prolonged increase of vascular permeability in *FoxM1* CKO lungs following LPS challenge. It is possible that there may have been greater lung vascular injury in *FoxM1* CKO mice; however, we observed similar increases in lung vascular permeability in CKO and WT mice within 6 hours of LPS challenge (time of peak increase in vascular permeability). The extent of endothelial cell apoptosis and neutrophil sequestration in lungs of WT and *FoxM1* CKO mice was also the same; thus, differences in apoptosis and neutrophil infiltration are not likely causes of the prolonged increase in lung microvascular permeability seen in *FoxM1* CKO mice. It is also possible that augmented production of proinflammatory mediators accounts for the defective endothelial repair in FoxM1-CKO mice. Our data also exclude this possibility, as *FoxM1* CKO and WT lungs expressed these mediators (e.g., IL-1β, TNF-α, IFN-γ, macrophage inflammatory protein-1α [MIP-1α], and monocyte chemoattractant protein-1 [MCP-1]) to the same degree following LPS challenge. Based on the findings that *Tie2* promoter/enhancer-driven *Cre* expression can cause gene deletion in endothelial cells as well as hematopoietic cells (31), it is possible that defective endothelial repair is the result of deletion of the FoxM1 gene in hematopoietic cells and failure of these cells to restore endothelial barrier function. However, we observed that FoxM1 was expressed in the bone marrow white blood cells of *FoxM1* CKO mice at the same levels as in WT mice both basally and following LPS challenge. To rule out the possibility that FoxM1 expression was defective in a small subpopulation of hematopoietic cells of *FoxM1* CKO

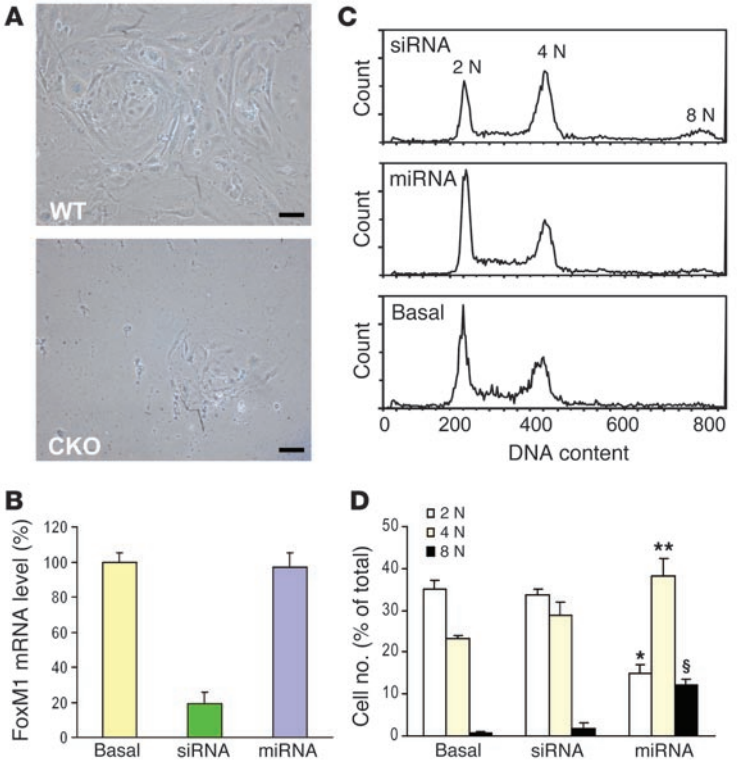

Figure 9
Defective cell cycle progression in FoxM1-deficient endothelial cells. (**A**) Representative micrographs of primary cultures of lung endothelial cells isolated from either 2-week-old WT or *FoxM1* CKO mice. Phase contrast pictures were taken at day 6 following isolation and culture. Scale bars: 50 μm. Growth of *FoxM1* CKO endothelial cells was severely reduced, and cell death was noted after 3–5 days in culture compared with WT cultures. (**B**) QRT-PCR demonstrated an approximately 80% decrease in levels of FoxM1 mRNA in HMEC-1 transfected with FoxM1 siRNA. Data are expressed as mean ± SD, $n = 3$. HMEC-1 were transfected with either 100 nM of siRNA (siRNA) against human FoxM1 or its cognate mutant siRNA (miRNA) or PBS (basal). At 65 hours after transfection, cells were collected for RNA isolation. (**C**) Cell-cycle profiles of HMEC-1. At 72 hours after transfection, cells were fixed and stained with propidium iodide. Representative FACS analyses of cell cycle profiles in asynchronous HMEC-1 are shown. (**D**) Graphic representation of accumulation of 4 N DNA content and increase of polyploid cells (8 N) in FoxM1-deficient endothelial cells. Data are expressed as mean ± SD, $n = 4$. $^{*}P < 0.01$ siRNA versus either basal or miRNA; $^{**}P < 0.05$ siRNA versus either basal or miRNA; $^{§}P < 0.05$ siRNA versus either basal or miRNA.

mice, WT bone marrow cells were transplanted into lethally irradiated *FoxM1* CKO mice. We found these reconstituted mutant mice still exhibited the sustained increase in vascular permeability at 48 hours after LPS challenge; thus, hematopoietic cells do not appear to be responsible for the defect seen in lung endothelial repair in *FoxM1* CKO mice following vascular injury.

Our results support the hypothesis that endothelial injury induces the activation of a FoxM1-regulated program mediating endothelial cell proliferation and restoration of endothelial barrier integrity. We found FoxM1 mRNA was induced in lungs of WT mice at day 2 and the value peaked at day 3 following LPS challenge, that is, precisely during the recovery phase of LPS-induced vascular injury. The expression of FoxM1 was also correlated with the rate of cell proliferation in lungs following vascular injury induced by LPS. There was a significant defect in endothelial barrier reannealing in *FoxM1* CKO lungs following LPS challenge, indicating that FoxM1 activation is critical for the restoration of endothelial integrity following lung vascular injury in mice.

To address whether cultured endothelial cells from *FoxM1* CKO mice also have defective cell cycle progression, we isolated primary mouse endothelial cells from *FoxM1* CKO lungs. These cells failed to proliferate normally, and many died after several days in culture. The suppression of FoxM1 expression in human microvascular endothelial cells using siRNA transfection also resulted in marked reduction in cell cycle progression. Our results documenting an important function of FoxM1 in restoration of endothelial integrity through its ability to promote cell proliferation are in agreement with the role of FoxM1 in regulating DNA replication and progression into and through mitosis (13, 14, 16, 17). Studies have demonstrated that FoxM1 regulates a network of genes essential for cell cycle progression in different cell types, including hepatocytes, mouse embryonic fibroblasts, and osteosarcoma U2OS (13, 14, 17–19). Our results are the first to establish the molecular basis of FoxM1-regulated proliferation of endothelial cells and vessel wall barrier repair.

We observed significant increases in protein levels of $p27^{Kip1}$ in *FoxM1* CKO lungs following LPS challenge and in FoxM1-deficient human endothelial cells. $p27^{Kip1}$ prevents Cdk phosphorylation of retinoblastoma (Rb) required for the activation of the E2F transcription factors and thereby inhibits cell proliferation (32). Its expression is reduced in endothelial cells in response to mitogenic factor, e.g., vascular endothelial growth factor (33). In addition, we observed significant decreases in Cdk1 and Cdk2 activities in FoxM1-deficient endothelial cells due to inhibition in the expression of cyclin-dependent kinase Cdc2 and multiple cyclins, including cyclins F, A2, B1, and D2. Cyclins and Cdks are key regulators of the cell cycle (34). Different cyclin-Cdk complexes are involved in regulation of specific cell cycle transitions: cyclin D–Cdk4/6 for G1 progression, cyclin E–Cdk2 for G1/S transition, cyclin A–Cdk2 for S phase progression, and cyclins A/B–Cdk1 for entry into M phase (34). Progression through G2/M transition requires the activation of the Cdk1–cyclin B complex through dephosphorylation and activation of Cdk1 by M phase tyrosine phosphatases Cdc25B and Cdc25C (35). Cdc25C functions as a concentration-dependent inducer of mitotic control, and it directs dephosphorylation of cyclin B–bound Cdc2 and triggers entry into mitosis (35). In FoxM1-deficient endothelial cells, Cdc25C expression was markedly decreased. These data provide a mechanism for the defect in proliferation of endothelial cells seen in *FoxM1* CKO mice. Thus, FoxM1 has an important role in regulating the expression of multiple genes essential for cell cycle progression in endothelial cells. In the absence of FoxM1, endothelial cells failed to proliferate, resulting in impaired recovery of endothelial barrier function.

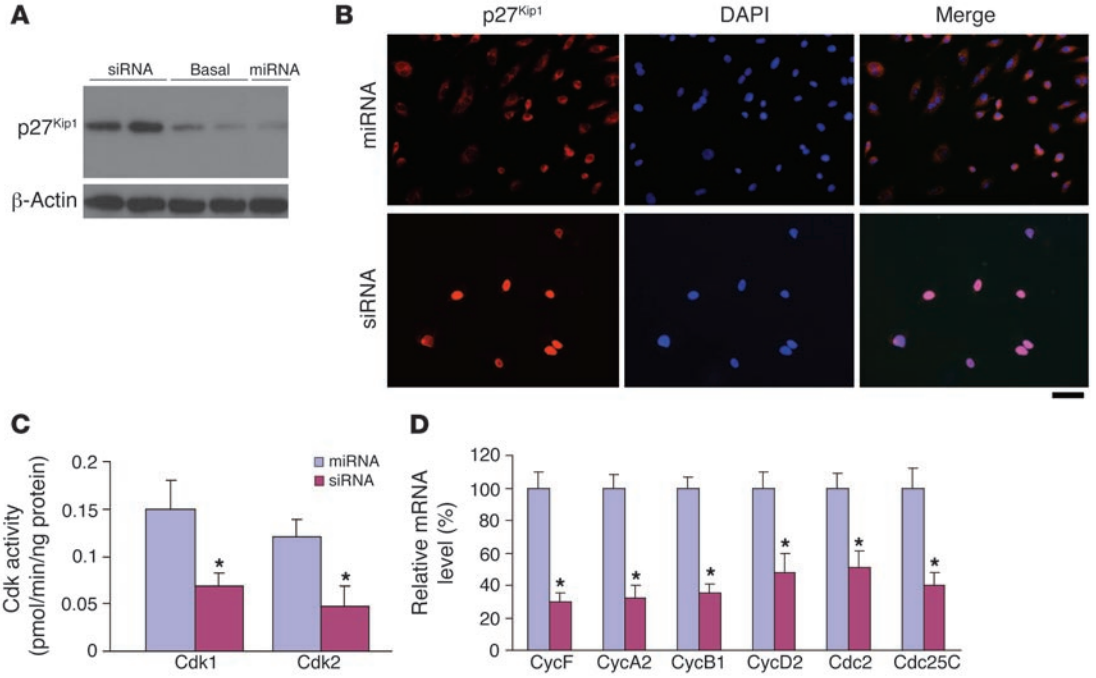

Figure 10

FoxM1 regulates expression of a network of genes essential for cell cycle progression in endothelial cells. (**A**) Increased expression of the cell cycle inhibitor p27^{Kip1} seen in endothelial cells following siRNA knockdown of FoxM1. HMEC-1 were transfected with either 100 nM siRNA against human FoxM1 (siRNA) or its cognate mutant siRNA (miRNA) or PBS (basal) for 72 hours, and protein lysates (50 μg/lane) were used for Western blotting. The experiment was repeated twice with similar results. (**B**) Representative micrographs of immunostaining of p27^{Kip1} in human microvascular endothelial cells. FoxM1-deficient endothelial cells exhibited extensive nuclear staining of p27^{Kip1}. Scale bar: 25 μm. (**C**) Graphic representation of decreased activities of Cdk1 and Cdk2 in FoxM1-deficient human microvascular endothelial cells. At 65 hours after transfection, cells were lysed for the Cdk activity assay. Data are expressed as mean ± SD, $n = 3$. *$P < 0.05$ versus miRNA. (**D**) QRT-PCR demonstrated decreased expression of cyclins, Cdc2, and Cdc25C in FoxM1-deficient human microvascular endothelial cells. At 65 hours after transfection, total RNA was isolated for QRT-PCR analysis. Cyclophilin mRNA levels were used for normalization. Data are expressed as mean ± SD, $n = 3$. *$P < 0.05$ versus WT. Cyc, cyclin.

In conclusion, the unperturbed vascular endothelium is normally quiescent and in a nonproliferative state. However, endothelial cells have the capacity to proliferate and reanneal the endothelial barrier after vascular injury. We provide evidence that the transcription factor FoxM1 is essential for the mechanism of endothelial cell proliferation following LPS-induced lung vascular injury and thereby plays a critical role in mediating endothelial barrier repair. Therefore, targeting FoxM1 activation to restore the restrictive nature of the vascular endothelial barrier may be a beneficial strategy for preventing lung inflammation associated with sepsis-induced ALI.

Methods

Mice. Endothelial cell–specific inactivation of *FoxM1* was achieved by cross-breeding *Tie2-Cre* transgenic mice with mice carrying the floxed *FoxM1* gene (13). In all experiments, littermates of genotypes of *FoxM1*$^{+/+}$, *FoxM*$^{fl/+}$, and *FoxM*$^{fl/fl}$ from the same breeding pair were used as WT while *FoxM1*$^{fl/fl}$ and *Cre* were used as *FoxM1* CKO. LPS (Sigma-Aldrich) at doses indicated was administrated by i.p. injection. All mice were bred and maintained in the Association for Assessment and Accreditation of Laboratory Animal Care–accredited animal facilities at the University of Illinois at Chicago according to NIH guidelines. Approval for animal care and use in these experiments was granted by the Animal Care and Use Committees of the University of Illinois at Chicago.

Molecular analysis. Total RNA was isolated using an RNeasy Mini Kit (QIAGEN), including DNase I digestion, and 1-step QRT-PCR analyses were performed in ABI Prism 7000 Sequence Detection System (Applied Biosystems). Dual-labeled (FAM/TAMRA; IDT probes were used for quantitative detection of expression of FoxM1 and FoxO1. The following primer/probe sets were used for analyses: mouse FoxM1, primers 5′-GGCGCACGGCGAAAG-3′ and 5′-TGGATGGGCACCAGGATAG-3′, probe 5′-(FAM)-TGAAGCCTCTGCTCCCTCGGGTT-(TAMRA)-3′; mouse FoxO1, primers 5′-CAAAGTACACATACGGCCAATCC-3′ and 5′-TGCTGTCCTGAAGTGTCTGCAT-3′, probe 5′-(FAM)-ATGAGCCCTTT-GCCCCAGATGCC-(TAMRA)-3′. Mouse cyclophilin primer/probe set was published previously (36). All gene expression was normalized to cyclophilin as an internal control. QRT-PCR analysis of expression of cyclins F, A2, B1 and D2, Cdc2, and Cdc25C was performed with QuantiTect SYBR Green PCR Kit (QIAGEN).

Western blot analysis was performed using p27^{Kip1} monoclonal antibody (1:1,000; BD Biosciences), and the same blots were reprobed with a β-actin antibody (C-2, 1:500; Santa Cruz Biotechnology Inc.) as a loading control.

Cdk1 and Cdk2 activity assays were performed as described (19). In brief, 300 μg of total cellular protein extracts from FoxM1 siRNA–treated or its cognate mutant–treated human lung microvascular endothelial cells were immunoprecipitated using a monoclonal antibody for Cdk1 (Upstate USA Inc.) or Cdk2 (Santa Cruz Biotechnology Inc.) overnight with gentle rocking at 4°C. Immunoprecipitated Cdk1 kinase was used for measurement of Cdk1 kinase activity with the Cdk1/Cdc2 kinase assay kit. Cdk2 kinase activity was measured with the same kit but using Cdk2-specific substrate and Rb amino acids 773–928 (Santa Cruz Biotechnology Inc.).

Cell proliferation and apoptosis assays. BrdU labeling and immunostaining were used to evaluate cell proliferation in mouse lung sections. BrdU (75 mg/kg BW) was injected i.p. into mice 4 hours prior to tissue collection. Mouse lung cryosections (3–5 mm) were stained with FITC-conjugated anti-BrdU following the manufacturer's instructions (In Situ Cell Proliferation Kit; Roche Diagnostics), and the nuclei were counterstained with DAPI. We used the In Situ Cell Death Detection Kit (Roche Diagnostics) for in situ apoptosis detection. Anti-vWF antibody (Sigma-Aldrich) was used to stain endothelial cells.

siRNA-mediated gene knockdown and cell cycle profiling. HMEC-1 were cultured in MCDB131 medium composed of 5% FBS, 10 ng/ml EGF, and 2 mM L-glutamine. Transfection of either siRNA against human FoxM1 or its mutant RNA duplex was performed with Lipofectamine 2000 (Invitrogen) at 50% confluence. Both siRNA and its mutant RNA duplex were synthesized based on published sequences (19). At 65 hours after transfection, total RNA was prepared for assessment of gene knockdown efficiency by QRT-PCR. At 72 hours after transfection, the cells were fixed with 70% ethanol and stained with propidium iodide for FACS analysis. Cell cycle profiling was performed by the FACS facility at the Research Resource Center at the University of Illinois at Chicago.

Primary cultures. Primary cultures of endothelial cells and nonendothelial cells were established using cells immunoselected from mouse lungs as previously described (37). In brief, a cell suspension was prepared from lungs by digestion with collagenase (1 mg/ml) and dispase (0.5 mg/ml) for 30 minutes twice, followed by filtration using 70-μm and 40-μm nylon filters. Endothelial cells were then selected using a rat antibody to mouse CD-31 (Chemicon International) and a secondary antibody coupled to magnetic beads (Miltenyi Biotec). Purified endothelial cells were plated on matrigel-coated 6-well plates and lysed for total RNA after growing 5–7 days in EBM-2 complete medium (Clonetics; Cambrex). Primary culture of nonendothelial cells was established by collecting cells from the endothelial cell–depleted flow-through of the magnetic column and plating on 0.2% gelatin–coated 10-cm dishes in DMEM composed of 10% FBS (Invitrogen). Confluent cultures of nonendothelial cells were then trypsinized and replated. Primary cultures of nonendothelial cells (fibroblasts and epithelial cells) at passage 4 were used for experiments.

Pulmonary microvascular permeability. Capillary $K_{f,c}$ was measured to determine pulmonary microvascular permeability to liquid as described (24). In brief, after the standard 30-minute equilibration perfusion, the outflow pressure was rapidly elevated by 13 cmH_2O for 3.5 minutes and then was returned to normal. The lung wet weight changed in a ramp-like fashion, reflecting net fluid extravasation. At the end of each experiment, lungs were dissected free of nonpulmonary tissue, and lung dry weight was determined. $K_{f,c}$ (ml/min/cmH_2O/dry g) was calculated from the slope of the recorded weight change normalized to the pressure change and to lung dry weight. As another approach to the assessment of the leakiness of pulmonary microvessels, we determined the rate of pulmonary edema formation by continuously monitoring the lung wet weight change. Lung weight changes of lungs obtained from different groups were followed until maximal edema or for 90 minutes after start of perfusion (24). Because the perfusate albumin concentration was constant at the onset of perfusion and pulmonary arterial pressure did not change during the 90-minute monitoring period, rate and magnitude of the increase in lung wet weight (i.e., attainment of a new isogravimetric state) provided another index of permeability of pulmonary microvessels).

Cytokine and chemokine expression profiles. Total protein was extracted from mouse lungs using RIPA buffer, and 25 μl of protein lysate (100–150 μg) was used to measure expression levels of the proinflammatory mediators, including IL-1β, TNF-α, IFN-γ, MIP-1α, and MCP-1, using the customer-selected mouse Bio-Plex Cytokine Assay (Bio-Rad). The assay was performed using the Bio-Plex System (Bio-Rad) following the manufacturer's instructions.

Bone marrow transplantation. Lethal irradiation was performed with a 6 MV photon beam from a linear accelerator. WT and *FoxM1* CKO mice (3 months old) were delivered a total of 1000 cGy at a dose rate of 100 cGy/min. At 3 hours following irradiation, the mice were transplanted with 1×10^7 isolated WT (*FoxM1*$^{fl/fl}$) bone marrow cells (200 μl of EBM2 medium) through tail-vein injection. To monitor the efficacy of reconstitution of bone marrow, bone marrow cells isolated from GFP transgenic mice were also transplanted into lethally irradiated *FoxM1* CKO mice. At 3 weeks after transplantation, bone marrow cells were isolated from these recipients and red blood cells were lysed. FACS analysis was performed to determine the percentage of the GFP-expressing population. In our protocol, an efficacy of at least 80% reconstitution was achieved. Five weeks after transplantation of WT (*FoxM1*$^{fl/fl}$) bone marrow cells, *FoxM1* CKO recipients were used for lung microvascular permeability measurement.

Statistics. Differences between groups were examined for statistical significance using Student's *t* test, except for statistical analysis in the mortality study following LPS challenge, which was performed with the Peto-Peto-Wilcoxon test. $P < 0.05$ denoted the presence of a statistically significant difference.

Acknowledgments

This work was supported by NIH grants T32HL007829, P01HL077806, and P01HL060678. We thank B. Kaushal and J.-S. Kim for their technical assistance.

Received for publication October 18, 2005, and accepted in revised form June 13, 2006.

Address correspondence to: Asrar B. Malik or You-Yang Zhao, Department of Pharmacology, University of Illinois College of Medicine, Chicago, Illinois 60612, USA. Phone: (312) 996-7635; Fax: (312) 996-1225; E-mail: abmalik@uic.edu (A.B. Malik). Phone: (312) 355-0238; Fax: (312) 996-1225; E-mail: yyzhao@uic.edu (Y.-Y. Zhao).

1. Cines, D.B., et al. 1998. Endothelial cells in physiology and in the pathophysiology of vascular disorders. *Blood.* **91**:3527–3561.
2. Ross, R. 1999. Atherosclerosis–an inflammatory disease. *N. Engl. J. Med.* **340**:115–126.
3. Libby, P., Ridker, P.M., and Maseri, A. 2002. Inflammation and atherosclerosis. *Circulation.* **105**:1135–1143.
4. Austin, G.E., Ratliff, N.B., Hollman, J., Tabei, S., and Phillips, D.F. 1985. Intimal proliferation of smooth muscle cells as an explanation for recurrent coronary artery stenosis after percutaneous transluminal coronary angioplasty. *J. Am. Coll. Cardiol.* **6**:369–375.
5. Schwartz, R.S., Holmes, D.R., Jr., and Topol, E.J. 1992. The restenosis paradigm revisited: an alternative proposal for cellular mechanisms. *J. Am. Coll. Cardiol.* **20**:1284–1293.
6. McFadden, E.P., et al. 1993. Response of human coronary arteries to serotonin after injury by coronary angioplasty. *Circulation.* **88**:2076–2085.
7. Ware, L.B., and Matthay, M.A. 2000. The acute respiratory distress syndrome. *N. Engl. J. Med.* **342**:1334–1349.
8. Kaestner, K.H., Knochel, W., and Martinez, D.E. 2000. Unified nomenclature for the winged helix/forkhead transcription factors. *Genes Dev.* **14**:142–146.
9. Clark, K.L., Halay, E.D., Lai, E., and Burley, S.K. 1993. Co-crystal structure of the HNF-3/fork head DNA-recognition motif resembles histone H5. *Nature.* **364**:412–420.
10. Korver, W., Roose, J., and Clevers, H. 1997. The winged-helix transcription factor Trident is expressed in cycling cells. *Nucleic Acids Res.* **25**:1715–1719.
11. Ye, H., et al. 1997. Hepatocyte nuclear factor 3/fork head homolog 11 is expressed in proliferating epithelial and mesenchymal cells of embryonic and adult tissues. *Mol. Cell. Biol.* **17**:1626–1641.
12. Yao, K.M., Sha, M., Lu, Z., and Wong, G.G. 1997. Molecular analysis of a novel winged helix protein, WIN. Expression pattern, DNA binding property, and alternative splicing within the DNA binding domain. *J. Biol. Chem.* **272**:19827–19836.
13. Wang, X., Kiyokawa, H., Dennewitz, M.B., and Costa, R.H. 2002. The Forkhead Box m1b transcription factor is essential for hepatocyte DNA replica-

tion and mitosis during mouse liver regeneration. *Proc. Natl. Acad. Sci. U. S. A.* **99**:16881–16886.
14. Kalinichenko, V.V., et al. 2004. Foxm1b transcription factor is essential for development of hepatocellular carcinomas and is negatively regulated by the p19ARF tumor suppressor. *Genes Dev.* **18**:830–850.
15. Kalinichenko, V.V., et al. 2003. Ubiquitous expression of the forkhead box M1B transgene accelerates proliferation of distinct pulmonary cell types following lung injury. *J. Biol. Chem.* **278**:37888–37894.
16. Krupczak-Hollis, K., et al. 2004. The mouse Forkhead Box m1 transcription factor is essential for hepatoblast mitosis and development of intrahepatic bile ducts and vessels during liver morphogenesis. *Dev. Biol.* **276**:74–88.
17. Laoukili, J., et al. 2005. FoxM1 is required for execution of the mitotic programme and chromosome stability. *Nat. Cell Biol.* **7**:126–136.
18. Costa, R.H. 2005. FoxM1 dances with mitosis. *Nat. Cell Biol.* **7**:108–110.
19. Wang, I.-C., et al. 2005. Forkhead box M1 regulates the transcriptional network of genes essential for mitotic progression and genes encoding the SCF (Skp2-Cks1) ubiquitin ligase. *Mol. Cell. Biol.* **25**:10875–10894.
20. Kisanuki, Y.Y., et al. 2001. Tie2-Cre transgenic mice: a new model for endothelial cell-lineage analysis in vivo. *Dev. Biol.* **230**:230–242.
21. Liao, Y., Day, K.H., Damon, D.N., and Duling, B.R. 2001. Endothelial cell-specific knockout of connexin 43 causes hypotension and bradycardia in mice. *Proc. Natl. Acad. Sci. U. S. A.* **98**:9989–9994.
22. Kondo, T., et al. 2003. Knockout of insulin and IGF-1 receptors on vascular endothelial cells protects against retinal neovascularization. *J. Clin. Invest.* **111**:1835–1842. doi:10.1172/JCI200317455.
23. Kim, I.M., et al. 2005. The forkhead box m1 transcription factor is essential for embryonic development of pulmonary vasculature. *J. Biol. Chem.* **280**:22278–22286.
24. Gao, X., et al. 2001. Differential role of CD18 integrins in mediating lung neutrophil sequestration and increased microvascular permeability induced by Escherichia coli in mice. *J. Immunol.* **167**:2895–2901.
25. Tiruppathi, C., et al. 2002. Impairment of store-operated Ca2+ entry in TRPC4(–/–) mice interferes with increase in lung microvascular permeability. *Circ. Res.* **91**:70–76.
26. Windsor, A.C., Mullen, P.G., and Fowler, A.A. 1993. Acute lung injury: what have we learned from animal models? *Am. J. Med. Sci.* **306**:111–116.
27. Ware, L.B., and Matthay, M.A. 2000. The acute respiratory distress syndrome. *N. Engl. J. Med.* **342**:1334–1349.
28. Fujita, M., et al. 1998. Endothelial cell apoptosis in lipopolysaccharide-induced lung injury in mice. *Int. Arch. Allergy Immunol.* **117**:202–208.
29. Kitamura, Y., et al. 2001. Fas/FasL-dependent apoptosis of alveolar cells after lipopolysaccharide-induced lung injury in mice. *Am. J. Respir. Crit. Care Med.* **163**:762–769.
30. Wiener-Kronish, J.P., Albertine, K.H., and Matthay, M.A. 1991. Differential responses of the endothelial and epithelial barriers of the lung in sheep to Escherichia coli endotoxin. *J. Clin. Invest.* **88**:864–875.
31. Koni, P.A., et al. 2001. Conditional vascular cell adhesion molecule 1 deletion in mice: impaired lymphocyte migration to bone marrow. *J. Exp. Med.* **193**:741–753.
32. Sherr, C.J., and Roberts, J.M. 1999. CDK inhibitors: positive and negative regulators of G1-phase progression. *Genes Dev.* **13**:1501–1512.
33. Abid, M.R., et al. 2004. Vascular endothelial growth factor activates PI3K/Akt/Forkhead signaling in endothelial cells. *Arterioscler. Thromb. Vasc. Biol.* **24**:294–300.
34. Massague, J. 2004. G1 cell-cycle control and cancer. *Nature.* **432**:298–306.
35. Nilsson, I., and Hoffman, I. 2000. Cell cycle regulation by the Cdc25 phosphatase family. *Prog. Cell Cycle Res.* **4**:107–114.
36. Zhao, Y.Y., et al. 2002. Defects in caveolin-1 cause dilated cardiomyopathy and pulmonary hypertension in knockout mice. *Proc. Natl. Acad. Sci. U. S. A.* **99**:11375–11380.
37. Frey, R.S., Rahman, A., Kefer, J.C., Minshall, R.D., and Malik, A.B. 2002. PKCzeta regulates TNF-alpha-induced activation of NADPH oxidase in endothelial cells. *Circ. Res.* **90**:1012–1019.